
LogGENE: A SMOOTH ALTERNATIVE TO CHECK LOSS FOR DEEP HEALTHCARE INFERENCE TASKS

A PREPRINT

Aryaman Jeendgar
BITS Pilani, Hyderabad Campus
jeendgararyaman@gmail.com

Aditya Pola
BITS Pilani
adityapola@gmail.com

Soma S Dhavala
ML Square
soma.dhavala@gmail.com

Snehanshu Saha
BITS Pilani, Goa Campus
snehanshus@goa.bits-pilani.ac.in

June 22, 2022

ABSTRACT

High-throughput Genomics is ushering a new era in personalized health care, and targeted drug design and delivery. Mining these large datasets, and obtaining calibrated predictions is of immediate relevance and utility. In our work, we develop methods for Gene Expression Inference based on Deep neural networks. However, unlike typical Deep learning methods, our inferential technique, while achieving state-of-the-art performance in terms of accuracy, can also provide explanations, and report uncertainty estimates. We adopt the Quantile Regression framework to predict full conditional quantiles for a given set of house keeping gene expressions. Conditional quantiles, in addition to being useful in providing rich interpretations of the predictions, are also robust to measurement noise. However, check loss, used in quantile regression to drive the estimation process is not differentiable. We propose log-cosh as a smooth-alternative to the check loss. We apply our methods on GEO microarray dataset. We also extend the method to binary classification setting. Furthermore, we investigate other consequences of the smoothness of the loss in faster convergence.

1 Introduction

A quantitative study of Gene Expression and its underlying regulatory mechanism is of inherent value in *curing diseases* like heterogeneous tumours and in controlling protein production for biotechnology purposes Zrimec et al. [2020]. This problem can be characterized in terms of understanding gene expression patterns of cells under various biological states. Diseases diagnosis and prognosis may be more broadly understood by measuring and observing changes in gene expression pattern. It might lead to better characterization of where, when and how genetic instructions are decoded in diseased cells and tissues. Sizeable publicly available datasets have been made available such as the *Connectivity Map* and the *Tor-21* project Mahadevan et al. [2011] towards such purposes. As a result, there is a surge in mining such gene expression datasets. A noteworthy application of this approach is to improve drug development success rates by screening vast libraries of compounds to affect and regulate the gene expressions patterns so as to restore the conditions found in healthy tissue Bai et al. [2013]. Neural networks have been applied for inferring Gene Expressions Eetemadi and Tagkopoulos [2018], Hanczar et al. [2020], most notably in Chen et al. [2016], and are used for modeling and simulations in drug development.

1.1 Our Approach

The patterns that the neural networks learn depend largely on the loss function used to drive the training process. As a result, choosing an appropriate loss function is very crucial. With that goal in mind, we pick the *Gene Expression* problem as a test bed for our experiments. We borrow the problem structure from Chen et al. [2016], where the gene expression problem was framed to predict the so-called *target genes* using already known *landmark genes*. These are a selection of 1000 genes that have been experimentally computed to be capturing up to 80% of the information contained in the entire genome. Prashanth et al. [2021] also used the same dataset to establish the utility of check loss. Hence, basing our experiments on this dataset to test our propositions would serve to 1. benchmark our proposed loss for fair comparisons 2. experimentally verify the theory of the log-cosh that we construct in the rest of the paper, on an important, large, real-world dataset.

2 Technical Motivation

The Mean Absolute Error (MAE) is a loss function of classical importance Huber and Ronchetti [2009] in robust Regression settings and is often preferred to Mean Squared Error (MSE) under heteroscedastic measurement-error regimes. Its asymmetric counterpart, the check loss (or pinball loss), is used in Quantile Regression. Majority of modern Machine Learning techniques only focus on predicting the conditional means, whereas with check loss, one could infer the entire conditional distribution, which is useful in quantifying the aleatoric uncertainty in the predictions. However, one severe drawback of using vanilla MAE or its extension in practice, particularly with deep neural networks, is its *non-differentiability*. With a renewed interest in exploiting first and second order derivatives in meaningful ways, Yao et al. [2021, 2020], Xu et al. [2018], Koh and Liang [2020], it is pragmatic to look for smoother alternatives to MAE and its extensions. Specifically, we suggest *log-cosh* as such an alternative to MAE and back this claim by providing relevant theoretical arguments and empirical validation on many data sets. Additionally, we consider the *Tilted log-cosh* rivalling the role of check loss in Quantile Regression. Later, *Tilted log-cosh* is adapted to Binary Classification settings to demonstrate its efficacy in learning latent conditional quantiles. We show how, in disease predictive modelling, such latent quantiles can augment explainability. In summary, our contributions are:

1. We prove relevant properties of the log-cosh that immediately follow in section-4
2. We provide a differentiable alternative to MAE, while retaining its statistical robustness. The intuition for the argument is developed in section-4.1.
3. We exploit the higher-order differentiability of the log-cosh by applying the L-BFGS optimizer on the GEO microarray dataset. The rationale, backed by our convexity proof, is explored in section-4.6
4. Extend *log-cosh* to the quantile regression and binary classification settings in section-4.7, so as to quantify the uncertainty of the predictions, instead of just point predictions.

A salient observation is how log-cosh lends itself to accomplish the above objectives simultaneously. As a result, our work lays an important foundation for building further. For example, Koh and Liang [2020] adapted Influence Functions (IFs) from Robust Statistics to Deep Learning setting. They can be used to fix labelling errors, provide counterfactuals, and identify out-of-distribution samples on gene networks, which could be extremely interesting. However, estimating IFs is fragile, and we hope that our work can alleviate some problems in this regard.

3 Related Work

Quantile Regression Koenker and Bassett [1978] in neural network settings has been explored in recent works. Schmidt-Hieber [2020], Padilla et al. [2020]. Moon et al. [2021] propose a constrained optimization approach for learning multiple non-crossing quantiles. Jantre et al. [2021] introduced a Bayesian neural network for quantile regression based on Asymmetric Laplace distribution (ALD). Notice that, in our work, when adapting the log-cosh to the Binary Classification setting, the response variables are modeled using the Hyperbolic Secant distribution, instead of ALD. Chen et al. [2016] propose a deep learning approach for gene expression inference, known as D-GEX. They posit the inference as a multi-task regression problem and considered a multi-layer feed forward neural network, trained with MSE loss. Since then, there have been multiple works exploring application of neural networks to the problem of Gene Expression Inference such as Eetemadi and Tagkopoulos [2018], Hanczar et al. [2020], Yuan and Bar-Joseph [2019]. On GEO microarray dataset, Prashanth et al. [2021] have applied quantile regression in the neural network setting, with Lipschitz Adaptive Learning rates. In our work, we recreate a subset of the results with tilted log-cosh (that offers a smooth alternative to the loss in Prashanth et al. [2021]) on the same dataset. Tambwekar et al. [2021] adapt the check loss to the binary classification setting. However, we show that tilted log-cosh may also be adapted to the binary

classification setting. Additionally, recent work Chen et al. [2019] has explored the applicability of the log-cosh to the generative domain as well.

The deep learning community have seen a recent resurgence in second-order optimization methods, With the emergence of better compute and tractability options, which were previously infeasible Yao et al. [2021, 2020], Xu et al. [2018], Koh and Liang [2020]. In our work, we show the applicability of L-BFGS Byrd et al. [1995], a standard second-order optimizer, on log-cosh.

4 Theoretical framework

4.1 Why the log-cosh

The fundamental intuition behind using the log-cosh as a plausible alternative to MAE is due to the following elementary observation. Consider:

$$\begin{aligned} \log(\cosh(x)) &= \log\left(\frac{e^x + e^{-x}}{2}\right) \\ &= \begin{cases} |x| - \log(2) & \text{large } x \\ \frac{x^2}{2} & \text{small } x \end{cases} \end{aligned}$$

This, in essence, tells us that the *log-cosh* behaves like the MAE asymptotically, which is the behaviour that we want in applications such as *Robust Regression* where the influence exerted by outliers in response is limited. Additionally, around the origin, log cosh behaves like MSE, retaining the statistical efficiency when measurement errors follow Normal distribution.

The above also captures our line of interest in the log-cosh as compared to *MSE*, *MAE* or its 'closest competitor', the *Huber* loss, which is defined as:

$$L_\delta(y, \hat{y}) = \begin{cases} \frac{1}{2}(y - \hat{y})^2 & |y - \hat{y}| \leq \delta \\ \delta(|y - \hat{y}| - \frac{1}{2}\delta) & \text{otherwise} \end{cases}$$

The Huber 'intuitively' combines the MAE and MSE in the same sense, but in a piece-wise manner. Like Huber, log-cosh can also be further parameterized, if desired, to control the transition from MSE to MAE-like behavior. Consider $\log \cosh(\frac{x}{h})$, where h can be tuned as per the needs of the application. For instance, if one wants more MAE-like behaviour, and the natural logarithm is used, then $h \approx 1$ is close to optimal, whereas for more MSE-like behaviour, $h \approx 0.7$ is close to optimal. Both MSE and MAE can be modeled as special cases. Hence, in that sense, it captures the same kind of convenience as the Huber in offering us a 'smooth' transition between the MAE and the MSE. At the same time, the log-cosh has the following properties that make it more appealing than Huber in the context of our applications:

1. The log-cosh has a tractable and well-studied generating distribution – the *Hyperbolic Secant distribution* – which allows a very convenient extension of the log-cosh to the non-parametric setting. Thus, adapting it for use in binary classification problems using neural networks becomes convenient.
2. Unlike the Huber, the log-cosh is arbitrarily differentiable *globally* (unlike the limited second-order differentiability of the Huber in the ' δ -basin' of its definition). Hence, the application of methods exploiting higher order differentiability is inevitably more stable for the log-cosh.

4.2 Convexity of the loss

In this section, we prove that the log-cosh is convex. Convexity of the loss is an immediately desirable quality because of the standard property of convex functions having a unique global minima and being much more "well-behaved" (Convexity implies local Lipschitzness). The latter is significant in ensuring a predictable, 'smooth' trajectory of the optimizer while navigating through the generated loss landscape. Our proof proceeds by first constructing the *Hessian* corresponding to the loss, and proving that it is *positive-definite*

Theorem 1 (log cosh is convex). *The log cosh is convex*

Proof. Consider $J = \sum_{i=1}^m \log \cosh(y_i - \theta^T x_i)$

$$\begin{aligned} J &= \sum_{i=1}^m \log \cosh(y_i - \theta^T x_i) \\ \frac{\partial J}{\partial \theta_\alpha} &= -\tanh(y^{(i)} - \theta^T x^{(i)}) x_\alpha^{(i)} \\ \frac{\partial^2 J}{\partial \theta_\alpha \partial \theta_\beta} &= \sum_{i=1}^m \operatorname{sech}^2(y^{(i)} - \theta^T x^{(i)}) x_\alpha^{(i)} x_\beta^{(i)} \end{aligned}$$

We construct the Hessian as: $H = XDX^T$ (with $D \equiv \operatorname{diag}(m \times m)$ and $D_{ii} = \operatorname{sech}^2(y^{(i)} - \theta^T x^{(i)})$)

Now, for some $u \in R^d$, consider the expression:

$$\begin{aligned} u^T H u &= u^T XDX^T u \\ &= \|D(X^T u)\|^2 \end{aligned}$$

Since $D_{ii} > 0$, we have $u^T H u > 0$, and hence the constructed Hessian is positive definite implying the convexity of the log cosh. \square

4.3 Lipschitzness

We would be interested in Lipschitzness of the log cosh from the perspective of a useful mathematical property and also to demonstrate the utility in developing an *Adaptive Learning Rate (LALR)* training regime. The latter builds on the Lipschitzness of the function Yedida et al. [2020] which is a consequence of convexity of log cosh. In this section, we prove that the log cosh is Lipschitz, and derive a tighter bound for the Lipschitz constant that we use in later experiments.

Lemma 1 (Lipschitzness of log cosh). *log-cosh is at least 1-Lipschitz*

Proof. It can be easily shown that, if the derivative of a differentiable function is bounded in a given domain by some ρ , then the function is ρ -Lipschitz – this follows directly from the definition of Lipschitzness and the *Mean-Value-Theorem*. Now, $\frac{d}{dx} \log \cosh(x) = \tanh(x)$. Since $|\tanh(x)| \leq 1$, log-cosh is *at least* 1-Lipschitz. \square

4.4 A tighter Lipschitz constant

Let us derive a more meaningful and *tighter* Lipschitz constant for the log-cosh. It should be noted that, Lipschitz constant is derived for the log cosh specifically in the *neural network* (regression) setting.

Theorem 2 (Tighter Lipschitz Constant of the log cosh). *log-cosh is Lipschitz, with a Lipschitz constant:*

$$\frac{1}{m} \tanh(g(0) - \|y\|) \cdot \max_j a_j^{[L]}$$

Proof. It can be shown that a valid Lipschitz constant for a loss function in the *Neural Net* setting may be obtained via the following expression - see equation (12) of Yedida et al. [2020]:

$$\max_{i,j} \left| \frac{\partial E}{\partial w_{i,j}^{[L]}} \right| \leq \max_j \left| \frac{\partial E}{\partial a_j^{[L]}} \right| \cdot \max_j \left| \frac{\partial a_j^{[L]}}{\partial z_j^{[L]}} \right| \cdot \max_j |a_j^{L-1}|$$

The first term on the RHS $\max_j \left| \frac{\partial E}{\partial a_j^{[L]}} \right|$, depends on our choice of the loss and is the main term that we will be spending

our time analytically computing. The second term: $\max_j \left| \frac{\partial a_j^{[L]}}{\partial z_j^{[L]}} \right|$, depends on our choice of the activation function, in the case of using ReLU activations (typical for the regression setting), this term can safely be taken to be equal to 1 (because gradient of ReLU only takes on a 0 or a 1, and we are taking a supremum over its range), or may be computed straightforwardly, depending on the activation that we choose to use for our networks. Finally, the third term has to be computed computationally, which is a really straightforward affair (we henceforth, refer to it as K_z). Hence, we now focus our efforts towards deriving an expression for the first term. The process for the same looks as below:

- First define the loss for the final layer:

$$E(\mathbf{a}^{[L]}) = \frac{1}{m} \log(\cosh(\mathbf{a}^{[L]} - \mathbf{y}))$$

- Now we write the derivative:

$$\frac{\partial E}{\partial \mathbf{a}^{[L]}} = \frac{1}{m} \tanh(\mathbf{a}^{[L]} - \mathbf{y})$$

- Now, we want to find where the parent equation for the lipschitz constant attains a maximum (and consequently, it's maximum value), for which we turn to it's second derivative (and points where it vanishes)

$$\begin{aligned} \frac{\partial E^2}{\partial^2 \mathbf{a}^{[L]}} &= \frac{1}{m} \operatorname{sech}^2(\mathbf{a}^{[L]} - \mathbf{y}) \\ \frac{\partial E^2}{\partial^2 w_{ij}^{[L]}} &= \frac{1}{m} \operatorname{sech}^2(\mathbf{a}^{[L]} - \mathbf{y}) \cdot K_z \\ \frac{\partial E^2}{\partial^2 w_{ij}^{[L]}} &= 0 : \text{ For computing the maximum} \end{aligned}$$

- Because sech remains non-zero, the only time the above second derivative vanishes is when $K_z = 0$, i.e. as per our definition, $a_i^{[L-1]} = 0$, which in turn implies, $z^{[L]} = w_{ij}^{[L]} a_i^{[L-1]} = 0$, hence finally yielding: $a^{[L]} = g(z^{[L]}) = g(0)$, finally giving us $\frac{\partial E}{\partial \mathbf{a}^{[L]}} = \frac{1}{m} \tanh(g(0) - \mathbf{y})$ (here, g , is the activation function) Now, notice that (can be seen algebraically for the $L-1$ norm):

$$\|\tanh(x)\| = \tanh(\|x\|)$$

The above, coupled with the simple triangular inequality for the 2-norm (i.e. imposing the 2-norm norm on both sides of the derivative equation) to obtain:

$$\frac{\partial E}{\partial \mathbf{a}_j^{[L]}} \leq \frac{1}{m} \tanh(g(0) - \|\mathbf{y}\|)$$

$$\boxed{\max_{i,j} \left| \frac{\partial E}{\partial w_{ij}^{[L]}} \right| = \frac{1}{m} \tanh(g(0) - \|\mathbf{y}\|) \cdot K_z} \quad (1)$$

where $\|\mathbf{y}\|$ is the maximum norm (across batches) of the labels. □

4.5 Robustness to Label noise

Another useful property of log-cosh as a loss function is that it is *robust to label noise*, meaning that the fluctuations in function output under small perturbations in its input has an upper bound. This places log-cosh on an equivalent setting as MAE. We state it formally below:

Lemma 2 (Robustness to label-noise). *log-cosh is robust to label noise.*

Proof. Mathematically, label noise resilience is captured as: $\|f(x + \epsilon) - f(x)\| \rightarrow 0$ as $\epsilon \rightarrow 0$ for some $\epsilon > 0$
Now, in our case: $f(x) = \log \cosh x$; $f(x + \epsilon) = \log \cosh (x + \epsilon)$. Consider:

$$\begin{aligned} \|f(x + \epsilon) - f(x)\| &= \|\log \cosh (x + \epsilon) - \log \cosh x\| \\ &= \left\| \log \left(\frac{\cosh (x + \epsilon)}{\cosh x} \right) \right\| \\ &= \|\log (\cosh \epsilon + \tanh x \cdot \sinh \epsilon)\| \end{aligned}$$

From the above, clearly, as $\epsilon \rightarrow 0$, $\|f(x + \epsilon) - f(x)\| \rightarrow \delta$ for some $\delta > 0$; $\delta \leq \epsilon$, and hence the theorem is established. □

4.6 Applications to second-order Optimization

Gradient Descent is the de-facto optimization method for neural network training, but there has been a recent interest Yao et al. [2021, 2020] in adapting some classical second-order methods to neural network optimization. The largest barrier to using 'vanilla' second-order optimization techniques (by and large are *Line-Search methods* Nocedal and Wright [2006]) are:

- Repeated computation of *Full Hessian* during backpropagation is not feasible. This can be alleviated to a certain extent by the use of *approximate* computations of the Hessian. Class of Quasi-Newton methods such as *L-BFGS* Byrd et al. [1995] is useful, which still retain the functional form of the Newton update.

- The Newton update doesn't readily lend itself for smoothing out noisy Hessian estimates. For first-order methods, there are several practical and well-developed methods for dealing with noisy gradient estimates like *Adam*. Some standard practices in neural network training like *Mini-batching* are also available. AdaHessian Yao et al. [2021], in the Deep Learning context, is one promising second-order method. However, it is very similar to Adam (AdaHessian essentially replaces the gradient with the diagonal of the Hessian in the Adam update).

As stated earlier, one of our objectives is also to test efficacy of log-cosh in second-order optimizers, for fitting the models. Is log-cosh a good candidate comparable to MSE? At the outset, MSE appears like an ideal candidate for the application of second-order optimizers, since line search methods in the case of quadratic objective functions are exact. However, this may not be the case with deep neural networks because of the inherent stochasticity and multi-modality, a very plausible scenario in the loss-landscape. Multi-modality, in the context of optimization, is defined here as the possibility of having multiple local minima and the absence of global minima in non-convex loss surfaces.

We choose to experiment with *L-BFGS* since the functional form of the update that the method uses is the same as the *Newton Update*, i.e. a step in the direction: $p_k = -B_k^{-1}\nabla f_k$, where B_k is the approximate Hessian constructed by the algorithm Nocedal and Wright [2006]. This ensures that the intuitive notion of steps in this direction being *exact* for the case of quadratic objective functions is retained (even if the *Hessian* that we use in this case is an approximation). As shown later, we observe in our experimentation with the L-BFGS and a 'large' neural network architecture, that the log-cosh performs significantly better than the MSE. Additionally, significantly less over-fitting can be seen in Figure-1. On classification and regression tasks, log-cosh is at least on par with other benchmark loss functions and optimizers.

4.7 Extension to the Binary-Classification setting

It is important to show that our proposed loss function can be readily extended to the binary classification setting. The following theorem formalizes the classification analogue of the tilted log cosh.

Theorem 3. *The Smooth Binary Quantile Classification Loss derived from the log-cosh is:*

$$\begin{aligned} L(y_i, \hat{y}_i) &= y_i \log(\hat{p}_i) + (1 - y_i) \log(1 - \hat{p}_i) \\ \hat{p}_i &= 1 - F_\tau(\hat{y}_i) \\ \hat{y}_i &= f_\tau(x_i) \quad \text{where, } f_\tau, \text{ is the latent function, the logits of the network} \end{aligned}$$

For any real valued random variable Z , with distribution function $F(z)$, with $F(z) = P(Z \leq z)$, the quantile function $Q(\tau)$ is given as $Q(\tau) = F^{-1}(\tau) = \inf\{r : F(r) \geq \tau\}$ for any $0 < \tau < 1$. Define τ as the marker for a typical Quantile loss. Then, the CDF, $F_\tau(\cdot)$ of f assumes the closed-form expression:

$$F_\tau(x) = \begin{cases} \tau + \frac{4\tau}{\pi} \tan^{-1}(\tanh(\frac{x}{2})) & x \leq 0 \\ \tau + \frac{4(1-\tau)}{\pi} \tan^{-1}(\tan(\frac{x}{2})) & x > 0 \end{cases}$$

Proof. Let $L(x)$ be the loss function with x being the input to the loss function. Then for the symmetric version of the loss function,

$$L(x) = \log(\cosh(x)) = \begin{cases} \log_e\left(\frac{e^x + e^{-x}}{2}\right) & x \geq 0 \\ \log_e\left(\frac{e^x + e^{-x}}{2}\right) & x < 0 \end{cases} \quad (2)$$

The asymmetric version of the loss function $L(x)$ can be obtained by tilting the loss as follows:

$$L(x) = \begin{cases} (1 - \tau) \log(\cosh(x)) & x < 0 \\ \tau \log(\cosh(x)) & x \geq 0 \end{cases}$$

Let $f(x)$ be the probability density function (PDF) and $F(x)$ be the cumulative density function (CDF), corresponding to $L(x)$, i.e.,

$$f(x) \propto e^{-L(x)}$$

The PDF can be obtained, after some routine calculus, as:

$$f(x) = \frac{2}{\pi} \operatorname{sech}(x) (\tau (\mathbb{1}_{x < 0}) + (1 - \tau) (\mathbb{1}_{x \geq 0}))$$

It can be easily verified that $\int_{-\infty}^0 f(x)dx = \tau$ which retains the interoperability that 0 is the τ -th quantile under this distribution. Further, $f(x)$ can be recognized as the *Hyberbolic Secent* distribution at $\tau = 0.5$. We can obtain CDF $F(x)$ using standard computations as:

$$F(x) = \begin{cases} \tau + \frac{4\tau}{\pi} \tan^{-1}(\tanh(\frac{x}{2})) & x < 0 \\ \tau + \frac{4(1-\tau)}{\pi} \tan^{-1}(\tanh(\frac{x}{2})) & x \geq 0 \end{cases}$$

□

Note: τ is the marker for Quantile losses which can be extended from $\text{logcosh}(x)$, making this loss interpretable as well. For example, $\tau = 0.5$ gives us the median i.e. MAE and L, L', L'' are well-defined for $\tau = 0.5$. Thus, at $\tau = 0.5$, the smooth, quantiled version of MAE i.e $\text{logcosh}(x)$ is continuous and twice differentiable and interpretable in the sense of binary quantile regression and binary quantile classification Tambwekar et al. [2021]

4.8 Lipschitzness of the sBQC loss

Smooth Binary Quantile Classification Loss, defined above, is also Lipschitz. In the following theorem, we provide a tighter bound for the Lipschitz constant, which is used in *LALR* training regime.

Theorem 4 (Lipschitz constant for the sBQC). *The Binary Smooth Quantile Classification Loss has the Lipschitz constant:*

$$\frac{2}{\pi} \max\left(1, \frac{1-\tau}{\tau}, \frac{\tau}{1-\tau}\right)$$

Proof. We may write the sBQC loss as:

$$L(y, z) = -(y \log p_z + (1-y) \log p_z)$$

where

$$p_z \equiv \begin{cases} 1 - \tau - \frac{4\tau}{\pi} \tan^{-1}(\tanh(\frac{z}{2})) & z \leq 0 \\ 1 - \tau - \frac{4(1-\tau)}{\pi} \tan^{-1}(\tanh(\frac{z}{2})) & z > 0 \end{cases}$$

We define: $\Delta L(y) \equiv \frac{|L(y, z_2) - L(y, z_1)|}{|z_2 - z_1|}$ – we may easily break down the computation in the case of Binary Classification problems into several pieces, which we deal with on a case-by-case basis as follows:

Case-1a: $0 < z_1 < z_2, y = 1$:

$$\Delta_z L(1) = \frac{\log(1 - \tau - 4(\frac{1-\tau}{\pi}) \tan^{-1}(\tanh(\frac{z_2}{2}))) - \log(1 - \tau - 4(\frac{1-\tau}{\pi}) \tan^{-1}(\tanh(\frac{z_1}{2})))}{z_2 - z_1}$$

The RHS in the above expression will take up a maximum value (which is what we want in the case of a Lipschitz constant) for $z_2, z_1 \rightarrow 0$, first imposing $z_1 \rightarrow 0$.

$$\lim_{z_2 \rightarrow 0} \Delta_z L(1) = \frac{\log(1 - \tau - 4(\frac{1-\tau}{\pi}) \tan^{-1}(\tanh(\frac{z_2}{2}))) - \log(1 - \tau)}{z_2}$$

which finally reduces to:

$$\lim_{z_2, z_1 \rightarrow 0} \Delta_z L(1) = -\frac{2}{\pi}$$

Case-1b: $0 < z_1 < z_2, y = 0$, Following the same structure as above, we get:

$$\lim_{z_2 \rightarrow 0} \Delta_z L(0) = \frac{\log(\tau + 4(\frac{1-\tau}{\pi}) \tan^{-1}(\tanh(\frac{z_2}{2}))) - \log \tau}{z_2}$$

which reduces to:

$$\lim_{z_2, z_1 \rightarrow 0} \Delta_z L(0) = \frac{2 - 2\tau}{\pi \tau}$$

Case-2a: $z_1 < 0 < z_2, y = 1$,

$$\lim_{z_2 \rightarrow 0} \Delta_z L(1) = \frac{\log(1 - \tau - 4(\frac{1-\tau}{\pi}) \tan^{-1}(\tanh(\frac{z_2}{2}))) - \log(1 - \tau)}{z_2}$$

Which reduces to:

$$\lim_{z_2, z_1 \rightarrow 0} \Delta_z L(0) = \frac{-2}{\pi}$$

Case-2b: $z_1 < 0 < z_2, y = 0$,

$$\lim_{z_2 \rightarrow 0} \Delta_z L(0) = \frac{\log(\tau + 4(\frac{1-\tau}{\pi}) \tan^{-1}(\tanh(\frac{z_2}{2}))) - \log \tau}{z_2}$$

which reduces to:

$$\lim_{z_2, z_1 \rightarrow 0} \Delta_z L(0) = \frac{2 - 2\tau}{\pi\tau}$$

Case-3a: $z_1 < z_2 < 0, y = 1$,

$$\lim_{z_2 \rightarrow 0} \Delta_z l(1) = \frac{\log(1 - \tau - 4(\frac{\tau}{\pi}) \tan^{-1}(\tanh(\frac{z_2}{2}))) - \log(1 - \tau)}{z_2}$$

which reduces to:

$$\lim_{z_2, z_1 \rightarrow 0} \Delta_z l(1) = \frac{2\tau}{\pi(\tau - 1)}$$

Case-3b: $z_1 < z_2 < 0, y = 0$,

$$\lim_{z_2 \rightarrow 0} \Delta_z L(0) = \frac{\log(\tau + 4(\frac{\tau}{\pi}) \tan^{-1}(\tanh(\frac{z_2}{2}))) - \log(\tau)}{z_2}$$

which reduces to:

$$\lim_{z_2, z_1 \rightarrow 0} \Delta_z l(1) = \frac{2}{\pi}$$

Hence, cumulatively, we may write the Lipschitz constant of the sBQC loss as:

$$\max\left(\frac{2}{\pi}, \frac{2 - 2\tau}{\pi\tau}, \frac{2\tau}{\pi(\tau - 1)}\right)$$

□

4.9 Regularization

Finally, we describe a penalty term that needs to be added to classification/regression loss. To that end, we specify that our model can be rewritten as:

$$y = I(z \geq 0), z = Q_x(\tau) = f_\tau(x) + \epsilon$$

where $\epsilon \sim HSD(\tau)$ and $HSD(y; \tau) = \frac{2}{\pi} \operatorname{sech}(y) [\tau I(y < 0) + (1 - \tau) I(y \geq 0)]$. The network learns the underlying latent function represented by $Q_x(\tau)$. When multiple quantiles are fit separately, it may be possible for lower quantile to be greater than an upper quantile – known as quantile crossing. The following regularizing term penalizes such quantile crossing:

$$L_{reg} = \sum_{i=1}^n \sum_{p=1}^{m-1} \max(0, Q_{x_i}(\tau_p) - Q_{x_i}(\tau_{p+1}))$$

5 Experimental results

The code and data for reproducing the below results may be found at Anonymous [2022].

5.1 GEO Microarray dataset

Training methodology: We run tests on two, 2-layer fully-connected neural network architectures, both of which differed only in the size of their intermediate layers. The 'small' and the 'large' architecture have [300,300] and [1000,1000] as the size of their hidden layers respectively, with a dropout of 0.1 for each. The dataset has 943 *landmark genes*, which serve as the input features, and 4760 *target genes*, which are modelled as the output features. We compare *log-cosh* against *MSE* and *MAE*. Each model was run on different training regimens, namely, *Constant Learning Rate with Adam*, *Lipschitz Adaptive Learning Rate with Adam* and *L-BFGS* (only with Log-cosh and MSE). We train two fully-connected neural network architectures for all of the runs, differing in the sizes of their intermediate layers. Each experiment was run for 500 epochs each.

5.1.1 Results

The results yielded by our experiments allow us to draw insights into the superior performance of Log-cosh. Firstly, networks trained with Log-cosh and MSE consistently outperform MAE. Secondly, our expectation to have L-BFGS converge in fewer iterations compared to its first order counterparts because of the quadratic nature of the log-cosh (section-4.6). This is well-supported by the results in table-1. Finally, another interesting observation highlighted by the figure-1, is that MSE overfits to a substantially greater extent than Log-Cosh while using L-BFGS as our optimizer. A rigorous under-taking to investigate this aspect is deferred for future work. Nonetheless, we observe superior performance of log-cosh on 'large' architectures and data sets and at least, equivalent performance as the baselines provided for by the MSE and MAE results. These tests validate that the log-cosh is a valid (and sometimes better) alternative to both the MSE and MAE.

Loss	Optimizer	D-GEX(small)	D-GEX(large)
Log-cosh	Adam	0.6348	0.6777
	LALR-Adam	0.6355	0.60542
	LBFSG	0.5642	0.5490
MSE	Adam	0.6321	0.6809
	LALR-Adam	0.5937	0.5389
	LBFSG	0.5582	0.6273
MAE	Adam	0.6528	0.7152
	LALR-Adam	0.6520	0.6261

Table 1: RMSE on GEO microarray

Name	sBQC								BCE							
	Adam				LALR-Adam				Adam				LALR-Adam			
	CP	JI	F1	%Acc.	CP	JI	F1	%Acc.	CP	JI	F1	%Acc.	CP	JI	F1	%Acc.
Heart Disease	0.6553	0.7162	0.8346	82.78	0.5227	0.6506	0.7883	76.22	0.6058	0.6883	0.8153	80.32	0.5081	0.6103	0.7581	75.41
WBC	0.9067	0.8867	0.94	95.71	0.9304	0.9151	0.9556	96.78	0.8906	0.8679	0.9292	95.00	0.9154	0.8981	0.9463	96.07
Pima	0.4005	0.3790	0.5497	75.00	0.4215	0.4716	0.6410	76.29	0.3792	0.4238	0.5953	73.37	0.4411	0.4840	0.6523	73.70
Haberman	0.2067	0.2142	0.3529	79.67	0.2548	0.2558	0.4074	81.30	0.1787	0.2173	0.3571	80.48	0.3045	0.2631	0.4167	79.67
Ionosphere	0.6802	0.8241	0.9035	86.42	0.7031	0.81	0.8950	86.42	0.7193	0.8381	0.9119	87.85	0.7005	0.8118	0.8961	86.42
Sonar	0.5821	0.6964	0.8210	79.51	0.6186	0.6923	0.8181	80.72	0.5556	0.6842	0.8125	78.31	0.4792	0.6441	0.7835	74.69
Banknote	1.0	1.0	1.0	100.0	0.9927	0.9921	0.9960	99.63	1.0	1.0	1.0	100.0	0.9926	0.9921	0.9960	99.63

Table 2: Binary Classification Results

Name	Log-cosh			MSE			MAE	
	Adam	LALR-Adam	LBFGS	Adam	LALR-Adam	LBFGS	Adam	LALR-Adam
Abalone	3.3878	3.149	3.14386	3.3269	3.1982	3.1232	3.5371	3.1979
Boston	10.7078	9.9378	9.8665	9.7432	9.7171	9.7173	9.8886	10.1969
Concrete	17.1732	17.6689	17.6579	17.9485	17.6132	17.62085	17.9380	17.6980
Energy	10.8102	10.3885	10.2397	11.6565	10.2407	10.2499	10.3692	10.3747
Wine	1.083	0.8673	0.8371	1.0353	0.8590	0.8367	1.0783	0.9311

Table 3: Generalizing LBFGS to UCI Regression data: LBFGS not applicable to MAE (tabulates observed RMSE)

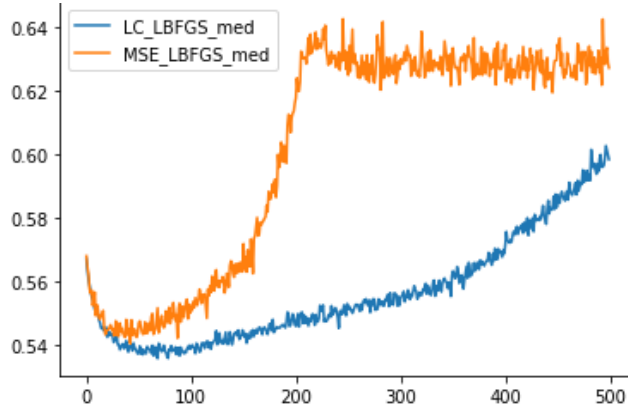


Figure 1: RMSE vs epochs for MSE and Log-Cosh trained using L-BFGS on the large architecture

5.2 Generalizability to other tasks

We also perform some testing on some standard UCI regression datasets to show that our method generalizes beyond just the GEO microarray dataset. These are collated in table-3. Root mean squared error (RMSE) on validation sets of various UCI regression datasets is reported. Log-cosh is compared against MSE and MAE while using three different optimizers namely, Adam (with constant learning rate), Adam (with LALR) and L-BFGS. Clearly, we observe that the log-cosh performs just as well as the MSE and MAE baseline results.

5.3 Binary Classification Problems

We use a standard three-layer neural network, with a hidden layer of size 100 for training the UCI binary classification datasets. We report *Cohen’s Kappa* (CP), *Jaccard index* (JI), *F1-score* and Accuracy. The *BCE* is used as the baseline for comparison against the proposed method, *sBQC*. *sBQC* exhibits superior performance on most of the classification tasks.

5.3.1 Model Evaluation

5-fold cross-validation is adopted on the data. We split the data into training and validation sets (80-20). These sets are selected such that their class distribution is representative of the original dataset (stratified k-fold). The training set is split into five-folds (one fold is used as test set), with the validation set being kept separate. This technique ensures that the models are not biased and the results are generalizable. Each fold was scrutinized carefully to check for no data leakage from the train set to the validation set, on all the runs.

Each experiment is run 20 times and the model is trained for 50 epochs in each run. The mean of the metrics under consideration is reported. We also report standard deviation values from the mean accuracy. The consistent performance of *sBQC* loss is apparent from the standard deviation in accuracy. The standard deviation values range from ± 0.17 to ± 0.87 which is reasonably small. The performance of *sBQC* and *BCE* was catalogued over the twenty runs and we find that on the Pima Indian diabetes, Wisconsin Breast Cancer(WBC), Cleveland Heart Disease and Haberman’s survival datasets, *sBQC* achieves better accuracy 17, 15, 16, 16 times respectively (the optimizer used for these runs was Adam with LALR).

5.4 Quantiles and Interpretability

This section aims to demonstrate a practical example of the explainability that learning multiple quantiles can offer. Using notation we introduced in 4.9, in a binary classification problem, we would be interested in observing for values of input the make latent function zero i.e. $z = 0$ (since that specifies our decision boundary). That involves solving the equation $Q_x(\tau) = 0$, in τ , for a fixed x . Assuming that we are able to solve the above equation for *any given* x we can make an important claim:

Given x being the value that the variable of interest takes on, and for the same τ being the solution to $Q_x(\tau) = 0$, at x , there is a $\tau\%$ chance that x would be classified as 0, and $(1 - \tau)\%$ chance as 1.

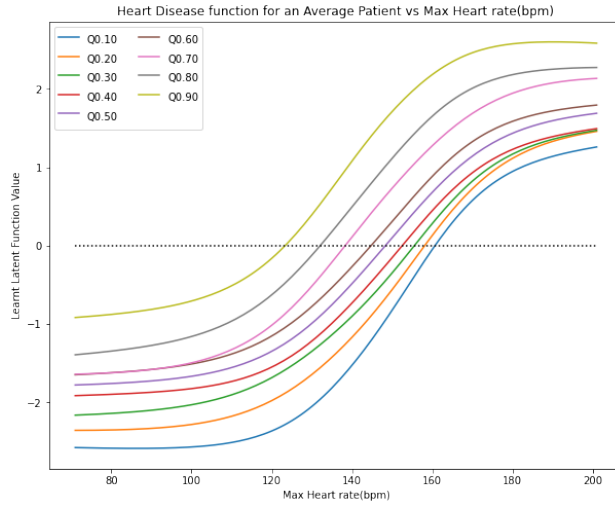


Figure 2: Multiple quantiles, heart-rate dataset

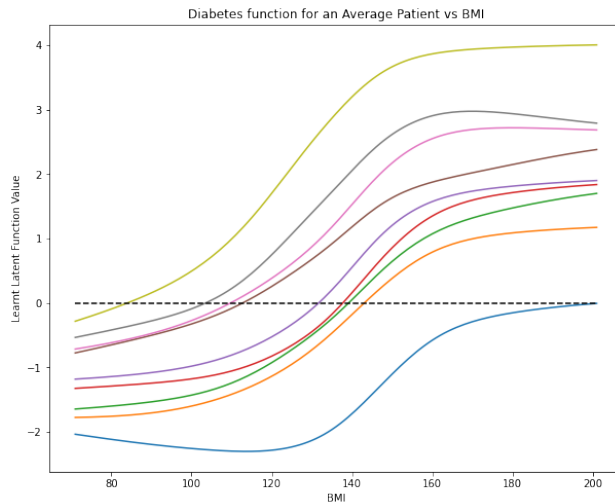


Figure 3: Multiple quantiles, Pima Indian dataset

For instance, we produce the above curve for the Heart Rate dataset where we used the log-cosh to learn the quantiles. An example reading of the curve would be: If there are two patients whose heart-rates are 120 BPM and 140 BPM, then there is a 90% and a 70% probability respectively, that the patients do not have heart-disease.

6 Impact towards AI for Good

Can gene expression inference techniques lead to cheaper drug design? A good precedence has been set already with leading Drug manufacturers like Pfizer and Genentech using AI powered solutions in their search for immuno-oncology drugs and cancer treatments. Efficient and accurate inference techniques are likely to produce quicker, cheaper and more-effective drug discovery leading to equitability in healthcare Fleming [2018]. We foresee the technique developed in the paper be used in a similar manner as DeepCE, an efficient Deep Learning based inference model Pham et al. [2021] which predicts correlations between gene expression and drug response. The method has helped identify drug re-purposing candidates for COVID-19 out of which two drugs (cyclosporine and anidulafungin) have received regulatory approval from FDA.

The UN Department of Social and Economic Affairs suggests 17 goals UN Dept. of Economic and Social Affairs [2015] which offers a systematized framework to achieve more equitable conditions of living. Developing computational and analytical models of gene regulations can contribute to one of the goals, which is to provide and improve *Good-Health and Well-Being*. Adopting a deep learning approach to this problem allows us to exploit the large amount of Gene Expression data. In addition, making these black-box models more explainable and robust is a significant step in the direction for harnessing the potential of Gene Expression data.

7 Conclusion

We have carried out extensive experiments to validate the claims made in the paper. Our experiments suggest that the log-cosh can be considered as an alternative to the MAE that can achieve state-of-the-art performance. Some of the properties such as Lipschitzness, differentiability, convexity, robustness *et cetera*, are useful in driving new training regimes. We explored the application of the L-BFGS optimizer. As we briefly discussed in the introduction, we are able to show via our experimentation on the GEO microarray dataset that the above stated properties of the *log-cosh* make it a model candidate for working with such sensitive data owing to the additional interpretability that we get out of quantiles. The benefits of such robust and smooth loss can be compounded in straightforward ways with the application of cutting-edge higher-order methods.

In summary, log-cosh accomplishes multiple objectives simultaneously in leveraging smoothness toward adaptive learning rates, providing smooth and robust alternatives to classical loss functions while offering higher order tractable alternatives to standard optimizers. Additionally, its binary classification analogue, the sBQC loss has been shown to achieve faster convergence due to its Lipschitzness, even against the similarly augmented BCE.

The current limitation of our work is the non-trivial extension of the sBQC loss to the multi-class classification setting, since there is no unique way to define the notion of multivariate quantiles. By extension, that would make our proposed sBQC loss much more attractive for application to image and text domains. Furthermore, exploration of the interplay between higher-order differentiability and quantiles is deferred to future work.

References

- Jan Zrimec, Christoph S. Börlin, Filip Buric, Azam Sheikh Muhammad, Rhongzen Chen, Verena Siewers, Wilhelm Verendel, Jens Nielsen, Mats Töpel, and Aleksej Zelezniak. Deep learning suggests that gene expression is encoded in all parts of a co-evolving interacting gene regulatory structure. *Nature Communications*, 11(1), December 2020. doi:10.1038/s41467-020-19921-4. URL <https://doi.org/10.1038/s41467-020-19921-4>.
- Brinda Mahadevan, Ronald D. Snyder, Michael D. Waters, R. Daniel Benz, Raymond A. Kemper, Raymond R. Tice, and Ann M. Richard. Genetic toxicology in the 21st century: Reflections and future directions. *Environmental and Molecular Mutagenesis*, 52(5):339–354, April 2011. doi:10.1002/em.20653. URL <https://doi.org/10.1002/em.20653>.
- Jane P. F. Bai, Alexander V. Alekseyenko, Alexander Statnikov, I-Ming Wang, and Peggy H. Wong. Strategic applications of gene expression: From drug discovery/development to bedside. *The AAPS Journal*, 15(2):427–437, January 2013. doi:10.1208/s12248-012-9447-1. URL <https://doi.org/10.1208/s12248-012-9447-1>.
- Ameen Eetemadi and Ilias Tagkopoulos. Genetic neural networks: an artificial neural network architecture for capturing gene expression relationships. *Bioinformatics*, 35(13):2226–2234, November 2018. doi:10.1093/bioinformatics/bty945. URL <https://doi.org/10.1093/bioinformatics/bty945>.
- Blaise Hanczar, Farida Zehraoui, Tina Issa, and Mathieu Arles. Biological interpretation of deep neural network for phenotype prediction based on gene expression. *BMC Bioinformatics*, 21(1), November 2020. doi:10.1186/s12859-020-03836-4. URL <https://doi.org/10.1186/s12859-020-03836-4>.

- Yifei Chen, Yi Li, Rajiv Narayan, Aravind Subramanian, and Xiaohui Xie. Gene expression inference with deep learning. *Bioinformatics*, 32(12):1832–1839, February 2016. doi:10.1093/bioinformatics/btw074. URL <https://doi.org/10.1093/bioinformatics/btw074>.
- Tejas Prashanth, Snehanshu Saha, Sumedh Basarkod, Suraj Aralihalli, Soma S Dhavala, Sriparna Saha, and Raviprasad Aduri. LipGene: Lipschitz continuity guided adaptive learning rates for fast convergence on microarray expression data sets. *IEEE/ACM Transactions on Computational Biology and Bioinformatics*, pages 1–1, 2021. doi:10.1109/tcbb.2021.3110516. URL <https://doi.org/10.1109/tcbb.2021.3110516>.
- Peter J. Huber and Elvezio M. Ronchetti. *Robust Statistics*. Wiley, 2 edition, 2009.
- Zhewei Yao, Amir Gholami, Sheng Shen, Mustafa Mustafa, Kurt Keutzer, and Michael W. Mahoney. Adahessian: An adaptive second order optimizer for machine learning, 2021.
- Zhewei Yao, Amir Gholami, Kurt Keutzer, and Michael Mahoney. Pyhessian: Neural networks through the lens of the hessian, 2020.
- Peng Xu, Farbod Roosta-Khorasani, and Michael W. Mahoney. Second-order optimization for non-convex machine learning: An empirical study, 2018.
- Pang Wei Koh and Percy Liang. Understanding black-box predictions via influence functions, 2020.
- Roger Koenker and Gilbert Bassett. Regression quantiles. *Econometrica*, 46(1):33, January 1978. doi:10.2307/1913643. URL <https://doi.org/10.2307/1913643>.
- Johannes Schmidt-Hieber. Nonparametric regression using deep neural networks with relu activation function. *The Annals of Statistics*, 48(4), Aug 2020. ISSN 0090-5364. doi:10.1214/19-aos1875. URL <http://dx.doi.org/10.1214/19-AOS1875>.
- Oscar Hernan Madrid Padilla, Wesley Tansey, and Yanzhen Chen. Quantile regression with deep relu networks: Estimators and minimax rates, 2020.
- Sang Jun Moon, Jong-June Jeon, Jason Sang Hun Lee, and Yongdai Kim. Learning multiple quantiles with neural networks. *Journal of Computational and Graphical Statistics*, 30(4):1238–1248, 2021. doi:10.1080/10618600.2021.1909601. URL <https://doi.org/10.1080/10618600.2021.1909601>.
- S. R. Jantre, S. Bhattacharya, and T. Maiti. Quantile regression neural networks: A bayesian approach. *Journal of Statistical Theory and Practice*, 15(3), June 2021. doi:10.1007/s42519-021-00189-w. URL <https://doi.org/10.1007/s42519-021-00189-w>.
- Ye Yuan and Ziv Bar-Joseph. Deep learning for inferring gene relationships from single-cell expression data. *Proceedings of the National Academy of Sciences*, 116(52):27151–27158, December 2019. doi:10.1073/pnas.1911536116. URL <https://doi.org/10.1073/pnas.1911536116>.
- Anuj Tambwekar, Anirudh Maiya, Soma Dhavala, and Snehanshu Saha. Estimation and applications of quantiles in deep binary classification, 2021.
- Pengfei Chen, Guangyong Chen, and Shengyu Zhang. Log hyperbolic cosine loss improves variational auto-encoder, 2019. URL <https://openreview.net/forum?id=rkg1vsc9Ym>.
- Richard H. Byrd, Peihuang Lu, Jorge Nocedal, and Ciyong Zhu. A limited memory algorithm for bound constrained optimization. *SIAM Journal on Scientific Computing*, 16(5):1190–1208, September 1995. doi:10.1137/0916069. URL <https://doi.org/10.1137/0916069>.
- Rahul Yedida, Snehanshu Saha, and Tejas Prashanth. Lipschitzlr: Using theoretically computed adaptive learning rates for fast convergence, 2020.
- Jorge Nocedal and Stephen J. Wright. *Numerical Optimization*. Springer, 2 edition, 2006.
- Anonymous. Code and data. shorturl.at/pPZ23, 2022.
- Nic Fleming. Nic fleming; nature(2018). <https://www.nature.com/articles/d41586-018-05267-x>, 2018.
- Thai-Hoang Pham, Yue Qiu, Jucheng Zeng, Lei Xie, and Ping Zhang. A deep learning framework for high-throughput mechanism-driven phenotype compound screening and its application to COVID-19 drug repurposing. *Nature Machine Intelligence*, 3(3):247–257, February 2021. doi:10.1038/s42256-020-00285-9. URL <https://doi.org/10.1038/s42256-020-00285-9>.
- UN Dept.of Economic and Social Affairs. The 17 goals | sustainable development. <https://sdgs.un.org/goals>, 2015.